ANS PSA 2013 International Topical Meeting on Probabilistic Safety Assessment and Analysis
Columbia, SC, September 22-26, 2013, on CD-ROM, American Nuclear Society, LaGrange Park, IL (2013)

SEAMLESS LEVEL 2/LEVEL 3 DYNAMIC PROBABILISTIC RISK ASSESSMENT CLUSTERING

Douglas M. Osborn, Tunc Aldemir, and Richard Denning
The Ohio State University
201 West 19th Avenue, Columbus, OH 43210

Diego Mandelli
Idaho National Laboratory
2525 Fremont Avenue, Idaho Falls, ID 83415

ABSTRACT

This paper discusses the work which has been conducted for a seamless Level 2/Level 3 dynamic probabilistic risk assessment (PRA) station blackout scenario for a series of MELCOR input decks for a 3-loop pressurized water reactor with a sub-atmospheric dry containment. This work is an extension of past dynamic PRA experiments and includes a Level 3 MELCOR Accident Consequence Code Systems, Version 2 (MACCS2) analysis. Various parameters within the MELCOR analysis have distributions (e.g. creep rupture) which can significantly affect the overall accident progression and environmental release. To further reduce conservatism, an updated containment fragility curve was incorporated. Since the amount of data produced from a dynamic PRA may be difficult to analyze using current Level 2 binning processes, the concept of 'data mining' provides a methodology to extract useful information. A post-processing tool has been developed by the Ohio State University to data mine using a mean-shift methodology to cluster scenarios. The scenarios are aggregated according to information on system components (e.g., valves fail to close) and system process variables such as pressure and temperature in the reactor coolant system. This post-processing methodology can be applied to aggregate scenarios after the Level 2 PRA analysis to determine common scenarios which can be analyzed in Level 3, or the methodology can be applied in the Level 3 PRA analysis thus carrying through all Level 2 PRA scenarios. For this work, the latter application of the methodology is considered.

Key Words: Dynamic PRA, Clustering, MELCOR, MACCS2

1 INTRODUCTION

The current approach to Level 2 probabilistic risk assessment (PRA) using the conventional event-tree/fault-tree methodology requires pre-specification of event order occurrence which may vary significantly in the presence of uncertainties. Manual preparation of input data to evaluate the possible scenarios arising from these uncertainties is a major source of analyst error from faulty/incomplete input preparation and their execution using serial runs represents a substantial computational challenge. A methodology has been developed for Level 2 analysis using dynamic event trees (DETs) that removes these limitations with systematic and mechanized methodology as implemented using the Analysis of Dynamic Accident Progression Trees (ADAPT) software.

For the work presented in this paper a seamless Level 2/Level 3 PRA station blackout scenario (long-term and short-term station blackouts were considered) using a DET analysis for a series of MELCOR input decks containing the Surry Power Station 3-loop pressurized water reactor (PWR) with a sub-atmospheric dry containment and the MELCOR deck is similar to that examined in NUREG-1935 [1]. This work is an extension of past ADAPT-MELCOR dynamic PRA [2-6] experiments and includes a Level 3 MELCOR Accident Consequence Code Systems,

Version 2 (MACCS2) analysis in which uncertainties in additional parameters are considered. Various parameters within the MELCOR analysis have distributions (e.g. creep rupture, safety relief valve failure, power recovery, hydrogen concentrations) which can significantly affect the overall accident progression and environmental release. To further reduce conservatism, an updated containment fragility curve was incorporated using data from NUREG/CR-5121 [1] and NUREG/CR-6920 [7].

1.1 Background

Past works such as WASH-1400 [8] and NUREG-1150 [9] used an event/fault tree approach for Level 1-3 PRA in a static time line. Between each level of PRA, plant damage states and core damage frequencies (Level 1 to Level 2), or large early release fraction (LERF), containment failure probability, source term quantification, particle size distribution, and released material energy (Level 2 to Level 3) were used to combine (binning) many similar scenarios into a few transitional inputs for subsequent level analysis. While this ground breaking work within the nuclear PRA provided insights that were never before recognized, it did have it limits, such as the inability to provide seamless transition between PRA levels, the lack of dynamic analysis, and limited sensitivity analyses.

When dynamic PRA is discussed in this paper, it is in reference to dynamic processes occurring within a nuclear reactor plant. These time-dependent processes are the basis upon which a dynamic event tree is created. Currently, dynamic PRA, such as that done with the software tool ADAPT, is designed to account for epistemic and aleatory uncertainties though DET generation. This type of dynamic PRA runs parallel DETs starting from a single initiating event, such as station blackout. The branching of the DETs occurs at user-specified times or when an action is required by the system (e.g., a valve or pump failure) or the operator. An example of this would be during a station blackout for a PWR, there is likelihood of failure for each steam generator safety relief valve (SRV). If SRV ‘A’ fails with a 5% failure probability and SRV ‘B’ fails with a 50% failure probability (i.e., 5%-A, 50%-B), it may not have the same outcome (i.e., timing within the accident sequence may not be the same for both SRVs to fail) if the failure probabilities for the SRVs were switched (i.e., 50%-A, 5%-B). Thus the two different scenarios may lead to completely different paths for system evolution. The evolution of the system to the next branching for these paths may occur at a different time, or may be based on different branching criteria. This dynamic method provides a major advantage over conventional event tree methods in that it more closely simulates reality.

For the purposes of this paper, aleatory uncertainties are defined as those arising from the stochasticity of the processes under consideration, such as the likelihood of rupture of a system within the framework of the PRA analyst who does not know the location or extent of flows in a vessel. Epistemic uncertainties are regarded as those arising from uncertainty in the model (i.e., system code) input parameters (e.g. heat transfer correlation parameters, friction coefficients, or the flow rate through a valve).

Other current dynamic PRA techniques account for epistemic and aleatory uncertainties through pure Monte Carlo sampling techniques, Monte Carlo DETs, or the ADS-IDAC approach [10-15]. Pure Monte Carlo sampling techniques and Monte Carlo DETs can account for dynamic progressions within the PRA analysis [10-13]. However, due to the nature of the randomness of the sampling process, these methods require repeating the runs for sensitivity studies on the choice of the probability distribution functions (pdfs) to represent the

uncertainties. The approach used in ADAPT uses a deterministic approach for the DET branching of scenarios along the uncertainty distribution. If it is later determined that the uncertainty distribution needs to be adjusted, the ADAPT approach allows for an adjustment in the uncertainty variable (i.e., adjusting the stochastic per demand failure probability for a safety relief valve at 5% is actually a 7.5% failure probability within a new uncertainty distribution) to be recalculated without the need to rerun the entire DET analysis. Monte Carlo sampling does not allow for this type of uncertainty distribution adjustment and will thus require a whole new DET analysis to be conducted.

The ADS-IDAC approach is similar to the ADAPT approach with respect to creating and monitoring DETs [14, 15]. However, the ADS-IDAC computational framework currently designed for one specific simulator, RELAP-5, and is limited to human interactions (e.g., procedural, knowledge based, or belief decisions) with the system. The ADAPT framework has an code-agnostic architecture that allows for easy replacement of simulators, component modules, and algorithms used in those components [16].

The approach employed in this paper uses ADAPT to develop the DETs which allows for a seamless transition from Level 2 to Level 3 without using the current practice of binning Level 2 results for the Level 3 analysis. Developing the branching and stopping rules for the calculations of radioactive material transport and release were a major challenge. Others have done binning determinations to investigate the important attributes of radioactive material transport [9, 10, 17, and 18]. However, the binning process is never an easy task since it is usually done within the post-processing of data, and can be limited in scope because of the limited number of scenarios analyzed. Using ADAPT, this research has the capability to investigate multiple low probability/high consequence scenarios which would normally be too costly and time consuming. The focus on low probability/high consequence scenarios will ensure that fewer scenarios are missed.

1.2 Objective and Computer Codes

The objective of this work is to extend the ADAPT [2, 18] methodology to combine Level 2 and Level 3 PRA. A seamless transition between Level 2 and 3 PRA can potentially reduce the magnitude of the source term uncertainty by removing the end states and binning process that is currently conducted when transitioning between Level 2 and Level 3. This research uses MELCOR [19] and MACCS2 [20] for source quantification and assessment of plume dispersion, respectively. The DETs cover all possible scenarios in the user-specified discretized uncertainty space and will be generated/evaluated in a mechanized fashion using distributed computing and intelligent scheduling through ADAPT to reduce analysis time and cost.

MELCOR was developed by Sandia National Laboratories (SNL) for the U.S. Nuclear Regulatory Commission (NRC) to model the progression of accidents in a light water reactor. A broad spectrum of accident phenomena in both PWRs and boiler water reactors (BWRs) can be treated with the code to estimate the fission product source term [19]. MELCOR can also be applied for sensitivity and uncertainty analyses within the estimated source term.

For this work, a series of MELCOR input deck for a PWR experiencing a station blackout [21] was investigated. The availability of AC electrical power is essential for the safe operation and accident recovery of a commercial nuclear power plant.

MELMACCS was developed by SNL to compile a MELCOR output and create a MACCS2 radionuclide input file. MELMACCS is a Windows based program that is used to create a MACCS2 source term input file from either a MELCOR Version 1.8.6 or Version 2.1 output plot file. This source term input file is only a part of the MACCS2 input deck. The other inputs for MACCS2 input deck are user-supplied.

The MACCS2 was developed by SNL for the NRC to simulate the release of a radiological plume to the atmosphere and estimate the consequences associated with the release. The code uses a segmented Gaussian Plume dispersion model and incorporates plume depletion, exposure pathway assessment and subsequent dose analysis. The current version of MACCS2, is used by commercial nuclear reactor companies, the NRC, and the U.S. Department of Energy for Level 3 PRAs, and radiological dose assessment for safety analyses and environmental studies. The current version of MACCS2 has a Windows based Graphical User Interface called WinMACCS.

The ADAPT code was developed by the Ohio State University as part of a SNL Laboratory Directed Research and Development project to generate dynamic event trees. A system simulator, such as MELCOR, can be linked with ADAPT to determine possible scenarios based on the branching and stopping rules provided by the user. ADAPT can keep track of scenario likelihoods and graphically display the DETs, as well as all simulator output as a function of time.

2 UNCERTAINTIES UNDER CONSIDERATION

For this work, 21 MELCOR input variables were assigned probability distributions. These input variables are the following:

- creep rupture of the stainless steel in the surge line,
- creep rupture of the stainless steel in the hot leg for loops A & C,
- creep rupture of the carbon steel weld joint between the reactor pressure vessel hot leg nozzle and the hot leg for loops A & C,
- creep rupture of the Inconel in the steam generator U-tubes for loops A & C,
- power recovery,
- hydrogen and carbon monoxide burn concentrations,
- failure of the turbine driven auxiliary feedwater pump (i.e., differentiates long-term and short-term station blackouts),
- failure of the DC station batteries,
- stochastic failure of a pressurizer SRV
- stochastic failure of a steam generator SRV (all loops were considered),
- high temperature cycling of a pressurizer SRV,
- high temperature cycling of a steam generator SRV (all loops were considered), and
- an application of a containment fragility curve.

Sections 2.1 through 2.7 describe how these uncertainties are accounted for in the seamless Level 2/3 PRA.

2.1 Creep Rupture

Equation 1 shows the creep-rupture failure model in which time to rupture, t_R, is determined with the following [19]:

$$t_R = 10^{(\frac{P_{LM}}{T} - C)} \quad (1)$$

where:

t_R = Time to rupture (seconds)

P_{LM} = Larson-Miller parameter

T = Temperature

C = Material property

P_{LM} is determined using the following equation [19]:

$$P_{LM} = \min[a_1 \log(\sigma_e) + b_1, a_2 \log(\sigma_e) + b_2] \quad (2)$$

where:

σ_e = effective stress

a_1, a_2, b_1, and b_2 = material property constants

The Larson-Miller parameter from Equation 1 and 2 is monitored by a MELCOR control function, LM-CREEP(t) using the following equation [19]:

$$LM\text{-}CREEP(t) = \int \frac{dt}{t_R(t)} \approx \sum \frac{\Delta t_i}{t_R(t_i)} \quad (3)$$

Usually when LM-CREEP(t) = 1 in Equation 3, MELCOR assumes that creep rupture occurs. However, the LM-CREEP(t) control function can allow for uncertainty within the Larson-Miller parameter to be investigated. This can be accomplished not by changing the Larson-Miller correlation, but by changing the LM-CREEP(t) value for rupture to be greater or less than 1.

For this particular work, only the 5%, 50%, and 95% percentile creep rupture parameters (i.e., 0518, 1.00, and 1.931 respectively) were used. The distribution used to select these data has been used in past work [3, 5, 16, and 18] and has been created using expert elicitation and experimental data for stainless steel, carbon steel, and Inconel creep rupture.

A parameter such as LM-CREEP(t) can be analyzed using the ADAPT approach by selecting points along a distribution. For example if the 5% probability was selected, the ADAPT approach executes the MELCOR code until LM-CREEP(t) = 0.518 upon where ADAPT would stop MELCOR, and create two branches. One branch will have LM-CREEP(t) = 0.518 and another branch will have LM-CREEP(t) > 0.518. Both of the daughter branches will then be restarted in MELCOR. For the branch in which LM-CREEP(t) > 0.518, a higher probability data point is selected and ADAPT will execute MELCOR until that new data point is reached. For the branch in which LM-CREEP(t) = 0.518, creep rupture occurs and ADAPT will allow MELCOR to execute until another branching stop point is achieved.

2.2 Power Recovery

As determined from past ADAPT work [2, 3], dynamic PRA analysis suggests that the timing of power recovery can be very important. Differences within power recovery timing as

little as ten minutes may result in completely different accident scenarios with major consequences such as late containment overpressure failure.

Control functions within MELCOR have been created in which AC power can be toggled on/off depending upon the power recovery scenario. For this work, it is assumed that the loss of the plant's loss of offsite power (LOOP) may be recovered but the loss of the plant's emergency diesel generators will not be recovered. The LOOP duration curves generated from NUREG/CR-6890 [21] are used for this research. Past ADAPT work [2, 3], used LOOP probabilities for "Critical Operations" because they have longer outage duration than those for "Shutdown Operations" and thus increase the probability of containment failure [21]. Based on data provided from this past ADAPT work "Critical Operation – Composite" durations of 1, 2, 4, 6, and 8 hours were selected.

For this work, a similar selection of "Critical Operation – Composite" duration times of 1, 4, and 8 hours as data points with corresponding probabilities of non-exceedance 47%, 84.3%, and 93.28% respectively.

2.3 Hydrogen and Carbon Monoxide Concentrations

The Hydrogen Combustion PRA model used in the original development of ADAPT [2, 3] allows for varying inputs of hydrogen (H_2) and carbon monoxide (CO) concentrations to be analyzed. The Three Mile Island Unit 2 (TMI-2) and Fukushima Daiichi multiunit accidents showed that hydrogen burn can (and in the case of Fukushima Daiichi Unit 1 and 3 will) occur during a severe accident. A hydrogen burn can create a pressure spike within containment that may be significant enough to cause containment rupture.

One way hydrogen is produced is within the reactor core as a result of a steam-zirconium reaction in which the zirconium (Zr) reacts with the oxygen (O_2) in the steam to produce zirconium oxide (ZrO_2) producing hydrogen. The reaction is described with the following reaction:

$$2\,H_2O + Zr \longrightarrow 2H_2 + ZrO_2$$

Hydrogen travels into containment through the pressurizer safety relief valves and ultimately through the reactor coolant system as a result of creep rupture.

An additional way hydrogen is produced is when the molten core, corium, comes into contact with concrete. Molten core-concrete interaction (MCCI) occurs after reactor pressure vessel failure and corium comes into contact with the concrete containment basemat. The high temperatures of the corium cause the water in the concrete to dissociate creating hydrogen and oxygen. Additional gaseous byproducts such as carbon dioxide and carbon monoxide are also produced during MCCI.

For hydrogen combustion to occur there must be a sufficient concentration of hydrogen and oxygen and the temperature of the reactants must be sufficiently high as well. There are many factors that determine if hydrogen combustion can occur and if it does occur will it propagate as a deflagration. The MELCOR Burn package does not allow for detonations to occur for combustion. A detonation is a combustion in which the flame front travels at supersonic speeds, while a deflagration flame front travels at subsonic speeds. While having the appropriate minimum concentrations of hydrogen and oxygen are important for combustion, steam (H_2O gas) and carbon dioxide (CO_2) are diluent gases that act as suppressers. If the diluent gases have

a combined concentration of ~55% of the containment atmosphere, hydrogen combustion cannot occur. Finally, a heat source is needed to act as an energy input for hydrogen combustion to occur. This is assumed to be the heat sources of the reactor coolant system.

During Power Recovery, the electrical equipment within containment may be energized and provide an additional ignition source for hydrogen. The Burn package within MELCOR has the capabilities to turn on/off these electrical ignition sources. Thus as part of the setup for the MELCOR/ADAPT runs, those ignition sources within containment are turned on/off depending on the specified Power Recovery scenario being investigated.

As the concentration of CO increases, the potential for a deflagration also increases [22]. CO is produced later in the accident scenario as a result of chromium metal from the reactor core attacking the containment concrete. This occurs when the reactor vessel lower plenum fails [23]. For CO combustion to occur there must be a sufficient concentration of CO and O_2 and the temperature of the reactants must be sufficiently high as well.

To determine the threshold for a deflagration to occur, LeChatelier's formula is used [24]. The Burn package in MELCOR uses the following equation provided the minimum concentration of O_2 is available, and the maximum concentration of diluent gases is not reached:

$$\frac{n(H_2)}{N(H_2)} + \frac{n(CO)}{N(CO)} \geq 1 \tag{4}$$

In Equation 4, *n* is the actual volumetric concentration for the specified gas (mole fraction) and *N* is the flammability limit for the specified gas (mole fraction).

A source of uncertainty in Equation 4 is the flammability limits of H_2 and CO [25-27]. Past ADAPT work [2, 3] has discussed experiments which provide different flammability limits for different test vessels and different deflagration flame propagation (upward or downward) [25]. Also, the temperature and pressure within containment can impact the flammability limits for H_2 [25-27].

For this work, the flammability limits are assumed to be normally distributed with a 10% mean standard deviation. The MELCOR default flammability limits for H_2 and CO are used as the means of, 0.10 and 0.167 mole fractions, respectively. Using Equation 2, the uncertainty in the flammability limits of N(H_2) and N(CO) are assumed to be represented by $1/N(H_2) = x$ and $1/N(CO) = y$. The mean values for x and y are $\mu_x = 1/0.10 = 10$ and $\mu_y = 1/0.167 = 5.99$ respectively. The corresponding 10% mean standard deviations are assumed to be $\sigma_x = 1.0$ and $\sigma_y = 0.599$ respectively. For $a = n(H_2)$ and $b = n(CO)$, it is well known from statistics that $z = ax + by$ also has a normal distribution with a mean of $\sigma_z = a\sigma_x + b\sigma_y$ and a variance of $\sigma^2_z = a^2\sigma^2_x + b^2\sigma^2_y$ and subsequent pdf [28]:

$$f(z) = \frac{exp\left(-\frac{(z-\mu_z)^2}{2\sigma_z^2}\right)}{\sigma_z\sqrt{2\pi}} \tag{5}$$

Then the cumulative distribution function (CDF) is:

$$F(z) = \int_0^\infty f(z)dz = \frac{1}{\sigma_z\sqrt{2\pi}} \int_0^\infty exp\left(-\frac{(z-\mu_z)^2}{2\sigma_z^2}\right) dz \tag{6}$$

which yields the probability P($z \geq 1$) for hydrogen burn (see Equation 4) as:

$$P(z \geq 1) = \int_1^{\infty} exp\left(-\frac{(z-\mu_z)^2}{2\sigma_z^2}\right) dz = \frac{1}{2}\left(1 - erf\left(\frac{1-\mu_z}{\sigma_z\sqrt{2}}\right)\right) \quad (7)$$

where the error function is:

$$erf(x) = \frac{2}{\pi}\int_0^x e^{-t^2} dt \quad (8)$$

Using Equations 4 through 8 produced a CDF for the flammability limits for H_2 and CO. For this work, the 5%, 50%, and 95% CDF points were selected for DET branching. This corresponds to 0.084, 0.10, and 0.116 mole fractions for H_2 respectively and 0.14, 0.167, and 0.194 mole fractions for CO, respectively.

2.4 Hydrogen and Carbon Monoxide Concentrations

For a station blackout (SBO) scenario, the steam turbine driven auxiliary feed water pump (TDAFWP) determines if the SBO will be a long-term station blackout (LTSBO) or a short-term station blackout (STSBO) event. If the TDAFWP starts at the initiation of the SBO, this can potentially extend the event and allow for a longer period of time for power recovery and thus prevent a failure of the primary system and ultimately the breech of containment (i.e. LTSBO). However, a LTSBO is also dependent upon having availability of the DC buses to monitor and control the TDAFWP as well (i.e., see Section 2.5 for a discussion on DC station batteries). If the TDAFWP is not available at the beginning of the SBO, then there is no way to provide make-up water to the steam generators. Thus there will be no heat sink for the primary system decay heat removal which in turns drastically reduces the time to primary system and containment failure.

An example of an extended SBO accident sequence was observed at Fukushima Daiichi Unit 2 and Unit 3. Both BWR plants have a steam driven system, reactor core isolation cooling (RCIC), to provide makeup water to the core and allow a heat sink for decay heat removal. In the SOARCA project for the integrated BWR plant analyses on the Peach Bottom Atomic Power Station, it was assumed that RCIC would fail over an hour after DC station batteries are exhausted (i.e., DC batteries are exhausted 4 hours into the unmitigated LTSBO event for the SOARCA Peach Bottom scenario) [29]. However, this was not the case for Fukushima Daiichi Unit 2 and Unit 3 RCIC operation. While not PWRs, these BWR accident sequences can provide insights into extended operating periods for emergency core cooling steam driven equipment (e.g., TDAFWP for PWRs and RCIC for BWRs).

For this work, the MELCOR/ADAPT analysis branches on whether the TDAFWP starts (LTSBO) or fails to start (STSBO) one second after the initiating event which causes a SBO. The probability of a LTSBO is assumed have a 90.91% change of occurrence. This was determined by assuming the core damage frequency of a LTSBO to be 2.0×10^{-5} per year and a STSBO core damage frequency of 2.0×10^{-6} per year [30].

2.5 DC Station Batteries

The DC station batteries are used for the DC electrical buses for minimum electrical loading to monitor instrumentation in the control room and for control of TDAFWP operations (i.e., see Section 2.4 for TDAFWP operations). For this work, it is assumed that the DC batteries will last an average of 4 hours. A normal distribution with a 50% mean standard deviation was assumed

for battery life. This resulted in a 5% CDF data point of 0.71 hrs and a 95% CDF data point of 7.29 hours for maximum lifetime battery usage.

2.6 Safety Relief Valves

All three steam generators and the pressurizer have multiple SRVs. The MELCOR model is setup to cause these SRVs to open at predetermined pressures and specified flow rates. The SRVs will close when pressure drops below 96% of their opening pressure. For the ADAPT/MELCOR model, each of the SRVs are set to fail open. The valve can fail open due to a stochastic per-demand failure probability (i.e., high number of cycles) or due to a set number of cycles above 1,000K (i.e., high temperature cycles).

To determine a CDF for the stochastic per-demand failure to close probability the following equation was used [28]:

$$P(n) = 1 - (1 - P_d)^n \tag{9}$$

where:

P_d = per-demand probability of failure to close

n = number of valve cycles

Equation 9 produces a CDF with an assumed per-demand failure probability of $P_d = 0.0027$, in which the 5%, 50%, and 95% probabilities were selected for this work. This selection corresponds to 19, 256, and 1,108 valve cycles, respectively.

The other SRV failure mode, high temperature cycling, is assumed to have the SRV stick to valve's backseat when steam flow temperatures are greater than 1,000K. For this failure mode, a uniform CDF was developed between 1 and 10 valve cycles. The 4%, 49%, and 81% CDF data points were selected because these points provide whole numbers. This corresponds to 2, 7, and 9 valve cycles respectively.

2.7 Containment Fragility Curve

Past research and scale model testing has been conducted on reinforced and pre-stressed concrete containments [7, and 31-33]. Through this testing, it has been determined that a concrete containment will start to leak before it fails due to rupture. This relationship has been coded into MELCOR and discussed in detail in NUREG/CR-6119 [19]. The leak rate will greatly increase once the containment's inner steel liner plate yields. This rate has been determined to be about 10 times more than the normal leak rate of 0.10% containment air mass per day at the containment's design pressure [7]. Once the rebar yields, the leak rate further increases to 13% [7]. Above this, a leak rate of 62% is observed for a global strain on the rebar of 1-2% after which there is no further significant increase in the global strain of the rebar [7]. However, the containment leakage rate will significantly increase with small increments in containment pressure rise [7].

For this work, two models were used to account for nominal leakage from containment and containment failure. Each model uses a MELCOR flow path adjusted to the containment pressure to accordingly simulate the leakage from containment to the environment. For the nominal leakage, the flow path is always active but very small. However, it should be noted that under normal operations the containment pressure is kept at a pressure less than atmospheric

pressure. This results in no leakage out of containment. It is not until there is a reactor accident that containment pressure can become greater than atmospheric pressure. The nominal leak rate is based off a 0.10% containment air volume per day leak rate when pressure, P, reaches design pressure, P_{Design} ($P/P_{Design} = 1$). Figure 1 provides a graphical representation of the nominal leak rate model [30].

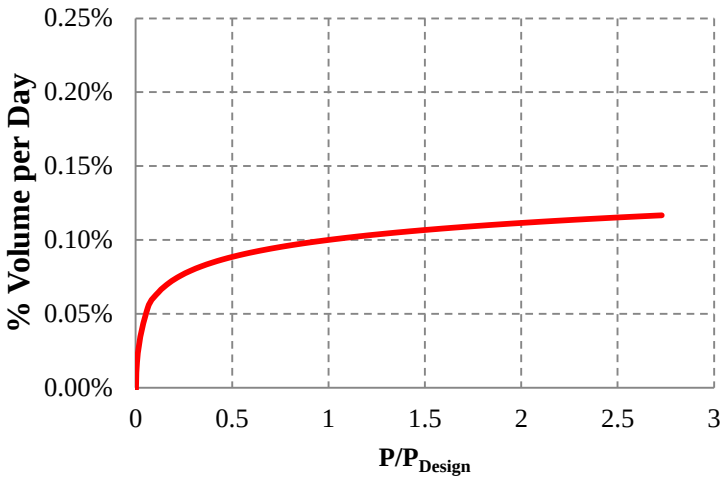

Figure 1. Nominal Containment Leakage

Based off of scale model testing [7, 33], it is assumed that containment failure begins once the rebar and containment inner steel plate liner yield. For this work, the containment failure model does not begin until P/P_{Design} reaches 2.175. Figure 2 shows the data points collected from NUREG/CR-5121 [7] (black data points) and the subsequent MELCOR containment failure model used to create a smoothed line (red line). Due to uncertainty in the leak rates obtained from these data points, a 15% reduction in the data was incorporated into the model.

Nominal leakage is seen to occur around areas of major penetrations such as the equipment hatch and the personnel airlocks [7, and 31-33]. These locations are where local strains are significantly higher than the global strains. For this work, it is assumed that both the nominal leak rate and the containment failure flow paths occur near the equipment hatch which is located near the mid-height of containment. For both models if the containment pressure decreases, the leakage area will not decrease from the maximum pressure value.

The data obtained in Figure 2 is assumed to be for a containment which is 99.99% reliable. Thus the data obtained for containment failure model in NUREG/CR-5121 can be combined containment fragility data obtained from NUREG/CR-6920 [8] to create a CDF containment fragility curve (CFC) shown in Figure 3. In Figure 3, the red line shows the minimum P/P_{Design} variable which will initiate the containment failure model and the green line denotes the design pressure ($P/P_{Design} = 1$). It was assumed that a P/P_{Design} of 2.175 was 99.99% of the distribution; the minimum data point in Figure 2. For this work, the 5%, 50%, and 95% distribution data

points were selected. This results in a P/P_{Design} of 1.235, 1.536, and 1.803, respectively. The data taken from NUREG/CR-6920 is for a release at mid-height of the containment. This allowed for a good fit between the data sets in NUREG/CR-5121 and NUREG/CR-6920.

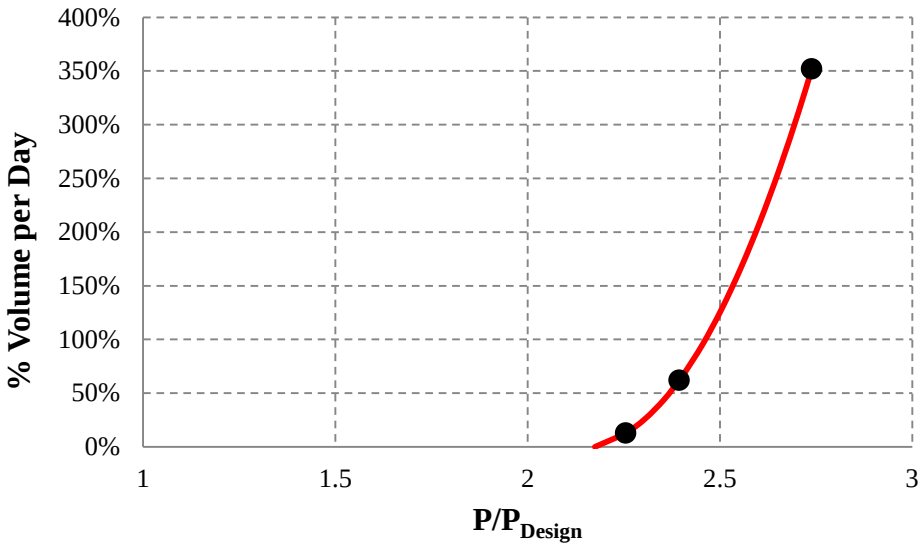

Figure 2. Containment Failure Leakage

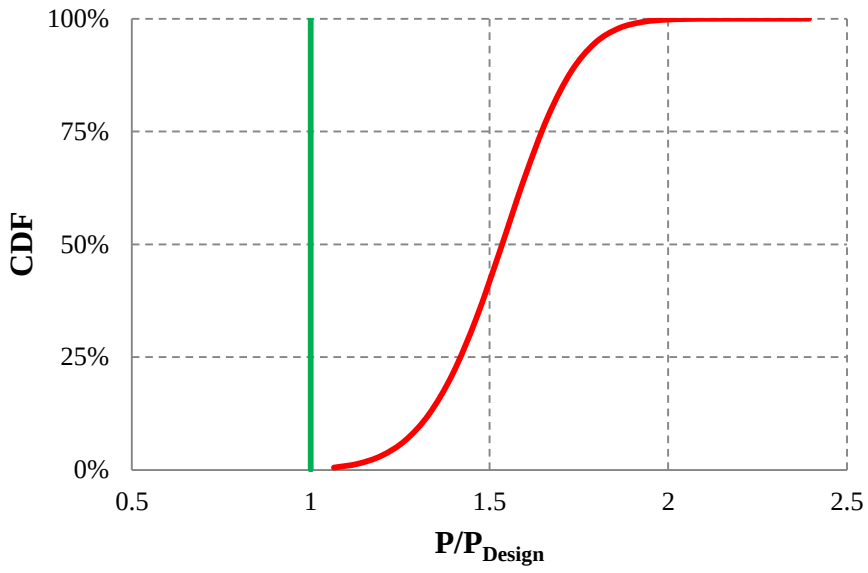

Figure 3. Containment Fragility Curve

3 DYNAMIC PRA CLUSTERING

Since the amount of data produced from a dynamic PRA may be difficult to analyze using current Level 2 binning processes, the concept of 'data mining' provides a methodology to extract useful information. A post-processing tool has been developed by the Ohio State University to data mine DETs using a mean-shift methodology to cluster scenarios. The scenarios are aggregated according to information on system components (i.e., valves fail to close or pumps fail to turn on) and system process variables such as pressure and temperature in the reactor coolant system. The aggregation of scenarios accomplishes two tasks:

- Identify the scenarios that have 'similar' behaviors (i.e. identify the most evident clusters), and
- Assign each scenario to a cluster (i.e. classification).

This methodology uses a non-parametric iterative mode-seeking procedure. The algorithm uses a hyper-dimensional sphere centered about a generic mean point with the radius of the sphere being called the bandwidth (BW). This allows the DET scenarios to be weighted during the estimation of the center of mass without losing any scenario information. Figure 4 provides an example of how this methodology reduces the DET scenarios from 446 individual scenarios, shown on the left, to five clusters, shown on the right. This methodology reduces the DET scenarios for the analyst into a more manageable analysis of scenarios and allows for better visualization of the data. Figure 4 shows that this methodology can allow for a single scenario to represent a cluster of scenarios and still allow a single out-layer scenario (i.e., from the legend, the '1' line on the right figure) to be differentiated from those scenarios that are more similar.

This post-processing methodology can be applied to aggregate scenarios after the Level 2 PRA analysis to determine common scenarios which can be analyzed in Level 3, or the methodology can be applied in the Level 3 PRA analysis thus carrying through all Level 2 PRA scenarios. For this work, the latter application of the methodology was considered.

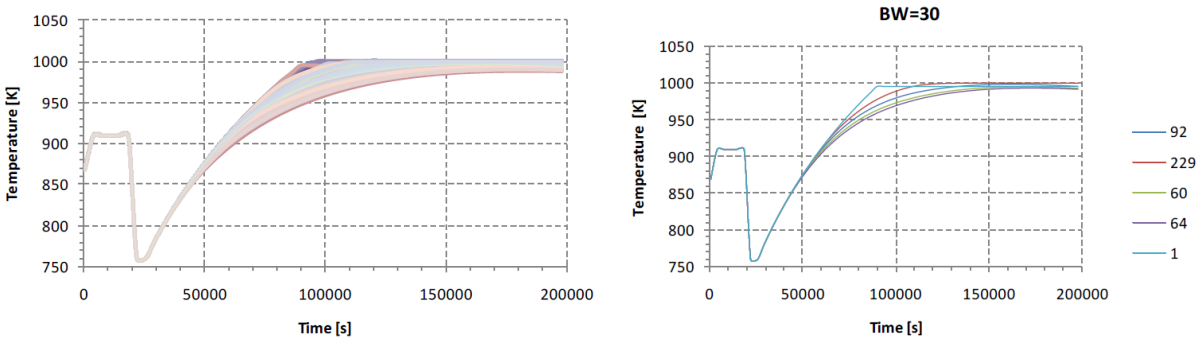

Figure 4. Scenario Reduction [5]

4 RESULTS

Prior to the SBO ADAPT/MELCOR initiating event, the PWR plant is assumed to be operating at 100% power with all essential subsystems working. The ADAPT/MELCOR simulations for the Level 2 PRA ran for 289 days which corresponds to 73.5 years of single MELCOR realizations. A total of 4,610 MELCOR realizations were produced and covered 95% of the total probability space for the 21 MELCOR input variables assigned probability distributions. Of these MELCOR realizations, 59% ran to completion and covered 91% of the total probability space. The other 49% of the MELCOR realizations failed due to code limitations (e.g., minimum time step limits were exceeded due to the COR package). However, these failed MELCOR realizations only covered 4% of the total probability space.

For the MELCOR realizations which ran to completion, 98% of the realizations resulted in some type of environmental release. However, these 2,657 MELCOR realizations only cover 2% of the total probability space. The other 51 MELCOR runs which ran to completion and cover 89% of the total probability space are SBO sequences with some type of power recovery which precludes environmental release, but do not necessarily preclude core damage. Thus, these 51 MELCOR realizations end within the Level 2 PRA analysis. A seamless Level 2/3 PRA was conducted for these 2,657 MELCOR realizations and resulted in 2,657 individual MACCS2 realizations.

4.1 ADAPT-MELCOR-MACCS2 Clustering

The MELCOR results are clustered based on 18 output variables. Table I provides a list of those variables. Based on these variables and the cluster technique discussed, 16 clusters of scenarios were created. For each of these clusters, the scenario nearest the mean of the cluster was selected to characterize the cluster. As noticed in Table I, some input parameters (e.g., the steam generator A Inconel Larson-Miller creep rupture parameter and the MACCS2 noble gas release path for primary-to-secondary leak) were excluded from the clustering parameters, based on the following observations:

- None of the 2,657 MELCOR scenarios with an environmental release was due to a thermally induced steam generator tube rupture. This is an unexpected result. In previous analyses, it was observed [1, 30] that under certain conditions for a STSBO with early failure of a stream generator SRV and a lower estimate of the Larson-Miller creep rupture parameter; a thermally induced steam generator tube rupture would occur. It was observed for all scenarios that the difference between the lower and upper bound of the Larson-Miller creep rupture distribution only varies the scenario by a few hours and once the Larson-Miller parameter for carbon or stainless steel reached 0.1, the Inconel parameter was still orders of magnitude lower.
- None of the ADAPT/MELCOR scenarios resulted in a thermal failure of the SRV. This was also an unexpected result. It was previously observed [1, 30] that under certain conditions for a SBO, high temperature gases would pass through a SRV which would lead to an earlier failure of the valve than would be estimated from the stochastic failure probability of multiple valve cycles.
- The TDAFW pump availability, which determines the difference a STSBO and a LTSBO, was not needed as a parameter for clustering. This is due to the differences in primary pressure signatures between a STSBO and a LTSBO due to the availability to

conduct a cooldown for LTSBO scenarios allowed the clustering technique to distinguish these scenarios without the use of the specific parameter.

- The battery life was not needed as a parameter for clustering. This is due to the differences in primary pressure signatures between a longer and shorter cooldown are captured in the clustering technique to distinguish these scenarios without the use of the specific parameter.

Table II provides the ADAPT/MELCOR branch identification number for the scenario nearest the mean, the number of scenarios within each cluster, and a generic description of each cluster. Additionally, Figure 5 provides an example, Cluster 1, of the clustering used for the 18 MELCOR output variables. It is apparent that all of the scenarios binned with this cluster have very similar transient behavior for this parameter. The other 15 clusters provide similar graphical representations of the output variables and were used to derive the generic cluster descriptions provided in Table II.

From Table II, it is discerned that ~0.8% of all scenarios had a stainless steel creep rupture of either the surge line, or one of the hot legs. Additional analysis into those ADAPT/MELCOR runs which failed to run to completion showed another 182 scenarios with stainless creep rupture (i.e., ~11% of all failed scenarios). However, the basis for these additional 182 stainless creep rupture scenario's failure cannot be determined to be a single cause failure within the MELCOR code. Thus, these and the other failed scenarios were not further analyzed. Additionally, none of the ADAPT/MELCOR runs which failed to run to completion showed a creep failure of the steam generator tubes. However, 26 scenarios did show a steam generator creep rupture parameter on the same order of magnitude (i.e., LM-CREEP ≥ 0.1) as the carbon steel creep rupture of the hot leg field weld or stainless creep rupture parameter that depressurized the reactor coolant system. It is likely that if a larger set of ADAPT/MELCOR cases were run to completion, some of those scenarios would have resulted in a steam generator tube failure.

As part of this work, a Level 3 PRA analysis was conducted using MACCS2. For every ADAPT/MELCOR case which produced an environmental source term, a MACCS2 analysis was conducted. In order to create a seamless transition between the Level 2 ADAPT/MELCOR outputs and the Level 3 MACCS2 inputs, MELMACCS was used. MACCS2 has the capability to calculate a number of offsite consequence measures. For the purposes of this study, we chose to use latent cancer fatality (LCF) risk as the metric. Results are provided conditional on the occurrence of the accident (i.e., conditional LCF risk). Thus, the results show the relative probability of different scenarios based on LCF risk. The LCF risk results are based on use of the linear-no-threshold dose-response model and are determined at 10-, 20-, 30-, 40-, and 50-mile radial distances from the plant.

None of the ADAPT/MELCOR cases produced any offsite fatalities, even for the population that is modeled as refusing to evacuate within the 10-mile emergency planning zone. All the MACCS2 reported values are expected (i.e., mean) values of the probability distribution obtained from a large number (i.e., approximately 12% of a year's worth of hourly weather data) of aleatory weather trials. The 'mean' MACCS2 values were used since only a single year of hourly weather data was used.

As part of the clustering methodology for the ADAPT/MELCOR/MACCS2 scenarios Level 2-to-Level 3 interface, the conditional and absolute LCF risk for each radial distance (i.e., 10-, 20-, 30-, 40-, and 50-mile radial distances were considered) was considered and

comparisons were conducted for each cluster. Figure 6 shows the complementary cumulative distribution function (CCDF) for the conditional LCF risk at specified radial distances. Figure 7 shows an example, Cluster 1, CCDF for conditional LCF risk to the overall CCDF conditional LCF risk at specified radial distances. As seen in Figure 7, Cluster 1 conditional LCF risk is in good agreement to the overall conditional LCF risk at the specified distances for the CCDF.

Table I. MELCOR Output Variables Used For Clustering

MELCOR Variable	Variable Name	Unit
CVH-P.160	Reactor Vessel Upper Head Pressure	Pa
CVH-P.5	Containment Basement Pressure	Pa
CVH-TVAP.110	Reactor Core Lower Head Temperature* (Atmospheric Temperature within control volume)	K
CVH-TVAP.201	Hot Leg A Temperature (upper node near RPV)	K
MACCS-01-M-RE-01	MACCS2 Noble Gas Release Path 1 (Containment Rupture)	kg
MACCS-02-M-RE-01	MACCS2 Noble Gas Release Path 2 (Containment Leakage)	kg
CFVALU.886	Surge Line Stainless Steel Larson-Miller Creep Rupture Parameter	unitless
CFVALU.869	Hot Leg A Carbon Steel Larson-Miller Creep Rupture Parameter	unitless
CFVALU.870	Hot Leg A Stainless Steel Larson-Miller Creep Rupture Parameter	unitless
CFVALU.849	Hot Leg B Carbon Steel Larson-Miller Creep Rupture Parameter	unitless
CFVALU.850	Hot Leg B Stainless Steel Larson-Miller Creep Rupture Parameter	unitless
CFVALU.829	Hot Leg C Carbon Steel Larson-Miller Creep Rupture Parameter	unitless
CFVALU.830	Hot Leg C Stainless Steel Larson-Miller Creep Rupture Parameter	unitless
CFVALU.9590	Maximum Containment H_2 Concentration	mol fraction
CFVALU.11212	Pressurizer SRV Stochastic Failure	cycles
CFVALU.16212	Steam Generator A SRV Stochastic Failure	cycles
CFVALU.17212	Steam Generator B SRV Stochastic Failure	cycles
CFVALU.18212	Steam Generator C SRV Stochastic Failure	cycles

*The hot leg is divided into two sections (upper/lower) for natural circulation

Table II. ADAPT/MELCOR/MACCS2 Clusters

Cluster Number	Number of Scenarios	ADAPT/MELCOR Branch ID	Scenario Description
1	471	10009	STSBO with carbon steel creep rupture and early pressurizer SRV failure
2	526	9348	LTSBO with carbon steel creep rupture and early pressurizer SRV failure
3	79	7530	STSBO with carbon steel creep rupture and early containment failure
4	948	9361	STSBO with carbon steel creep rupture
5	207	11316	LTSBO with carbon steel creep rupture
6	17	7841	STSBO with carbon steel creep rupture, early containment failure, and early pressurizer SRV failure
7	258	5759	LTSBO with carbon steel creep rupture and short DC battery life
8	8	4967	STSBO with carbon steel creep rupture at the upper end of the creep rupture distribution, early containment failure, early pressurizer failure SRV, and early steam generator SRV failure
9	5	4723	STSBO with carbon steel creep rupture at the lower end of the creep rupture distribution, early containment failure, early pressurizer failure SRV, and early steam generator SRV failure
10	14	11617	STSBO with stainless creep rupture and early steam generator B SRV failure
11	50	5761	STSBO with carbon steel creep rupture and early containment failure
12	2	5845	STSBO with stainless steel creep rupture and early pressurizer SRV failure
13	4	5898	STSBO with stainless creep rupture and early steam generator A SRV failure
14	66	8310	LTSBO with carbon steel creep rupture and early containment failure
15	1	6479	STSBO with carbon steel creep rupture, containment leakage only, and early failure of all steam generator SRVs
16	1	11393	STSBO with stainless steel creep rupture and containment leakage only

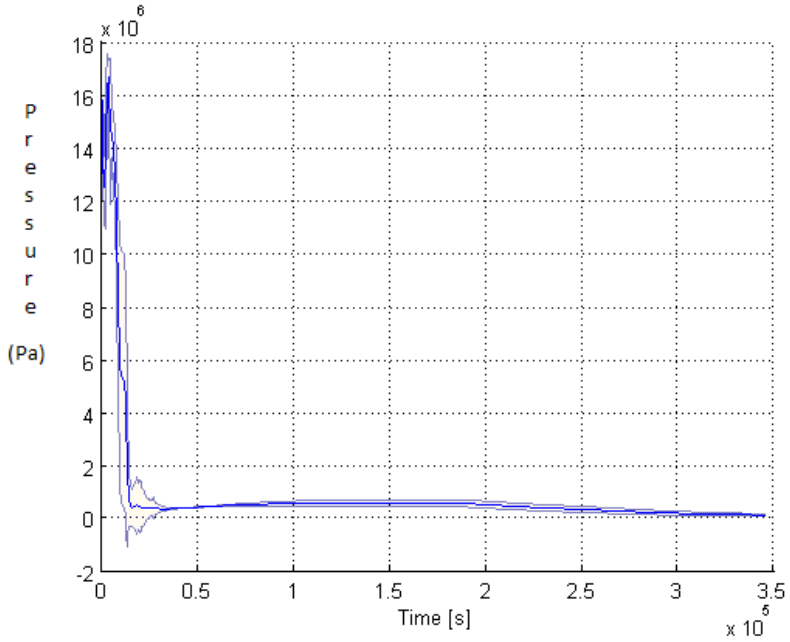

Figure 5. Reactor Vessel Upper Head Pressure for Cluster 1

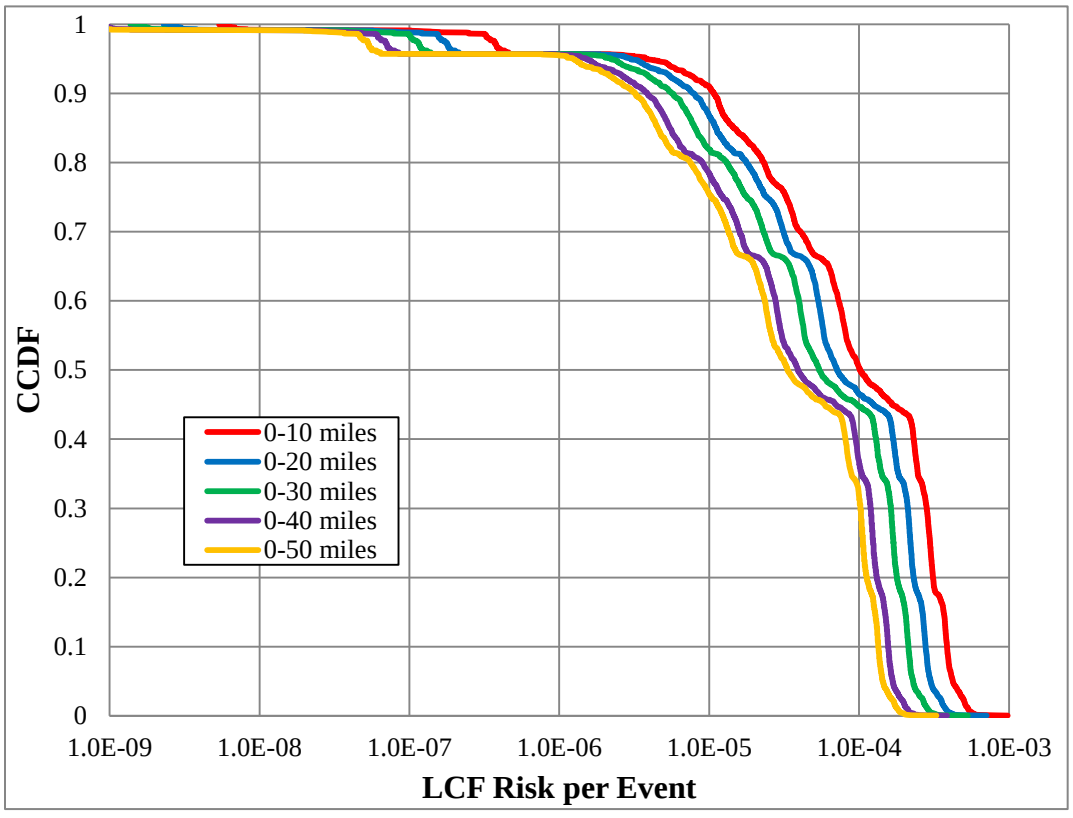

Figure 6. CCDF of Conditional LCF Risk at Specified Radial Distances

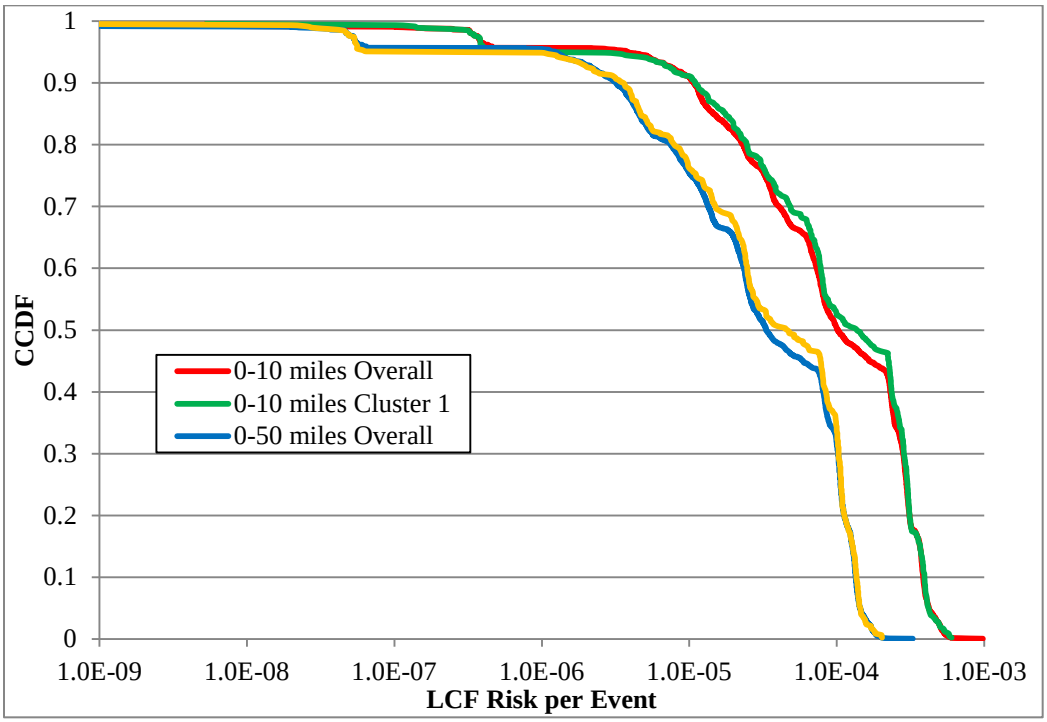

Figure 7. CCDF of Conditional LCF Risk for Cluster 1 and the Overall CCDF for Conditional LCR at Specified Radial Distances

4.2 Latent Cancer Fatality Comparison

For this analysis, a 'major' cluster is one which has more than 20 scenarios assigned to that cluster and represents the highest probability bins. Thus, 8 of the 16 clusters are considered major clusters and covers 99.7% of the environmental consequence probability. A comparison of the conditional and absolute LCF risk was conducted for the Level 2-to-Level 3 PRA interface. For each of the ADAPT/MELCOR/MACCS2 scenarios nearest the mean of each cluster (i.e., see Table II) the conditional and absolute LCF risk was compared with the mean for the conditional and absolute LCF risk for each cluster, respectively. Table III shows the 8 major clusters, how many scenarios are assigned to each cluster, and the difference between the mean cluster conditional LCF risk to the overall mean conditional LCF risk for all radial distances considered.

Based on the eight clusters from Table III, the mean conditional LCF risk is within each cluster is in good agreement to the overall mean conditional LCF risk, and further emphasizes the agreement seen in Figure 7 between a major cluster (e.g., Cluster 1) and the overall conditional LCF risk. These eight clusters over predict the overall mean by less than 11% and under predict the overall mean by less than 20%. Based on this determination and that these major clusters represent 99.7% of the scenarios which release to the environment, these clusters were chosen to determine the overall effectiveness of absolute LCF risk as an environmental consequence risk metric. For the ADAPT/MELCOR scenario nearest the cluster mean for the eight major scenarios, the ADAPT/MELCOR scenario under predicts the overall mean of the

conditional LCF risk 7 out of 8 times. Table IV provides the ADAPT/MELCOR scenario nearest the cluster mean and how they compare to the conditional LCF risk for each cluster. From Table IV, 7 of 8 ADAPT/MELCOR/MACCS2 scenarios shown in Table II are within an order of magnitude of the overall cluster mean and would thus be considered a good representation of the overall mean of conditional LCF risk if they were to be considered a single point estimate for a Level 2 to Level 3 PRA transition. This work indicates that the clustering technique using the 18 MELCOR variables provides a good representation of the conditional LCF risk; this is expected.

Table III. Cluster Comparison to the Mean, Overall Conditional LCF Risk

Cluster #	Total # of Scenarios	Difference between Cluster mean and Overall Mean ("+" the cluster over predicts the overall average)
1	471	4.0%
2	526	5.2%
3	79	-3.5%
4	948	-2.7%
5	207	4.5%
7	258	-4.1%
11	50	11%
14	66	-20%

Table IV. ADAPT/MELCOR Cluster Comparison to the Mean Cluster Conditional LCF Risk

Cluster #	ADAPT/MELCOR Branch ID	Difference to Cluster Mean ("+" over predicts the cluster mean)
1	10009	-99.86%
2	9348	-66%
3	7530	-40%
4	9361	57%
5	11316	-61%
7	5759	-91%
11	5761	-80%
14	8310	-24%

When absolute LCF risk was considered, a noticeable change occurred when the mean of each major cluster was compared with the overall mean of absolute LCF risk. As seen in Table V, only one major cluster (Cluster 14) was within 10% of the mean overall absolute LCF

risk, and half of the major clusters under predict the mean overall absolute risk by ~40% to 60%. This indicates that half the major clusters contribute to most of the absolute risk for LCFs (i.e., compare Table III and Table V). For the four major clusters where the mean is greater than the overall mean for absolute LCF risk, only Cluster 4 consistently produced absolute LCF risk results reflecting it's rank in Table V (e.g., the mean absolute risk for Cluster 4 is the highest when compared to the other major clusters). From Table II, Cluster 4 contains sequences resulting in a STSBO. Even though the conditional probability for a STSBO is an order of magnitude lower than the LTSBO, the STSBO Cluster 4 LCF risk is large enough to off-set this difference. This is unexpected considering recent work [1] would suggest that the absolute LCF risk for LTSBO scenarios would be dominate.

Table V. Cluster Comparison to the Mean, Overall Absolute LCF Risk

Cluster #	Total # of Scenarios	Contribution to the Overall Probability	Difference between Cluster mean and Overall Mean ("+" the cluster over predicts the overall average)
1	471	10.7%	-45%
2	526	12.3%	11%
3	79	4.1%	-58%
4	948	48.0%	30%
5	207	7.9%	-40%
7	258	8.9%	-39%
11	50	3.0%	20%
14	66	4.7%	3.0%

4.3 Latent Cancer Fatality Cluster Risk Comparison

Based on the initial assessment for conditional LCF risk, discussed in Section 4.2, it would seem the ADAPT/MELCOR/MACCS2 scenario selected for each cluster would be a good representation of the overall absolute LCF risk. However, when these scenarios were compared individually to the overall mean absolute LCF risk, they were poor predictors of the absolute LCF risk because their respective individual conditional probability is low. For this work, the overall mean absolute LCF risk was compared to the overall risk based on the cluster using the following equation is used to determine the overall cluster risk:

$$OCF = \sum_{x=1}^{16} \sum_{z=1}^{n} C_{z,x} * L_x \quad (10)$$

Where:

OCF = Overall cluster frequency

L_x = ADAPT/MELCOR realization conditional LCF risk for Cluster 'x'

$C_{z,x}$ = Conditional probability for realization 'z' in Cluster 'x'

z = ADAPT/MELCOR realization for a specified cluster

n = Total number of ADAPT/MELCOR realizations for Cluster 'x'

x = ADAPT/MELCOR Cluster

This comparison of the absolute LCF risk of the overall mean to overall cluster frequency result using Equation 10 yields a 40% over prediction when considering all clusters and a 48% under prediction when considering just the 'major' clusters. Further analysis showed that for Clusters 10 and 15, while only contributing 0.22% to the overall probability, consistently ranked the highest and third highest absolute risk for all environmental risk metrics, respectively (i.e., Cluster 14 is consistently ranked the second highest). Thus, these two clusters are what drive the over prediction for all the clusters. Yet, this comparison shows that when the clustered ADAPT/MELCOR/MACCS2 scenarios are considered for overall cluster frequency, the mean ADAPT/MELCOR/MACCS2 scenarios are indeed a good predictor of the overall mean absolute LCF risk.

5 CONCLUSIONS

A binning process was conducted using the clustering techniques described in Section 3. For this analysis, the ADAPT/MELCOR/MACCS2 scenario nearest the mean for each cluster was considered the source term which would be carried through to the Level 3 PRA analysis (i.e., see Table II). LCF risk was considered for both conditional and absolute risk. Based on this analysis, the following insight was gained regarding the current dynamic PRA clustering methodology:

- The ADAPT/MELCOR scenario nearest the cluster mean are within an order of magnitude of the overall cluster mean and would thus be considered a good representation of the overall mean of conditional LCF risk if they were to be considered a single point estimate for a Level 2 to Level 3 PRA transition. This work indicates that the clustering technique using the 18 MELCOR variables provides a good representation of the conditional LCF risk; this is expected.
- When the overall risk based on the cluster using the ADAPT/MELCOR scenario nearest the mean for each cluster is sufficient for the 18 MELCOR variables selected when absolute LCF risk is considered. The ADAPT/MELCOR scenario nearest the mean for each cluster over predicts the overall mean by 40%.
- The cluster with the highest mean absolute LCF risk, Cluster 4, contains sequences resulting in a STSBO. Even though the conditional probability for a STSBO is an order of magnitude lower than the LTSBO, the STSBO Cluster 4 LCF risk is large enough to off-set this difference. This is unexpected considering recent work [1] would suggest that the absolute LCF risk for LTSBO scenarios would be dominate.
- For the cluster technique considered, the parameters selected are typically used to understand the in-containment behavior of scenarios, and for this work, these parameters can be used as a surrogate for assessing absolute LCF risk to the public.

6 REFERENCES

1. U.S. Nuclear Regulatory Commission, NUREG-1935, "State-of-the-Art Reactor Consequence Analyses (SOARCA) Report," Washington D.C. (2012).

2. Hakobyan A., R. Denning, T. Aldemir. S. Dunagan, and D. Kunsman, "A Methodology for Generating Dynamic Accident Progression Event Trees for Level 2 PRA", *PHYSOR 2006*, Vancouver, Canada, September 10-14, Volume B034, pages 1-9 (2006).
3. Rutt B., U.V. Catalyurek, A. Hakobyan, K. Metzroth, T. Aldemir, R. Denning, S. Dunagan and D. Kunsman, "Distributed Dynamic Event Tree Generation for Reliability and Risk Assessment", *Proceedings of the International Workshop on Challenges of Large Applications in Distributed Environments (CLADE'06)*, IEEE Computer Society, Paris, France, June 19-23, pages 61-70, (2006).
4. Catalyurek, U., B. Rutt, et al., "Development of a Code-Agnostic Computational Infrastructure for the Dynamic Generation of Accident Progression Event Trees," The Ohio State University, Columbus, OH (2009).
5. Mandelli, D., A. Yilmaz, K. Metzroth, T. Aldemir, and R. Denning, "Scenario Aggregation and Analysis via Mean-Shift Methodology," *Proceedings for the 2010 International Congress on Advances in Nuclear Power Plants (ICAPP '10)*, San Diego, CA, June 13-17, Paper 10293, San Diego, CA (2010).
6. Hakobyan, A., T. Aldemir, R. Denning, et. al., "Dynamic Generation of Accident Progression Event Trees," *Nuclear Engineering and Design*, **Volume 238**, pages 3457-3467 (2008).
7. U.S. Nuclear Regulatory Commission, "Experimental Results from Pressure Testing a 1:6-Scale Nuclear Power Plant Containment," NUREG/CR-5121, U.S. Nuclear Regulatory Commission, Washington D.C. (1992).
8. U.S. Nuclear Regulatory Commission, "Risk-Informed Assessment of Degraded Containment Vessels," NUREG/CR-6920, U.S. Nuclear Regulatory Commission, Washington D.C. (2006).
9. U.S. Nuclear Regulatory Commission, "Reactor Safety Study – An Assessment of Accident Risks in U.S. Commercial Nuclear Power Plants," WASH-1400 (NUREG 75/014), U.S. Nuclear Regulatory Commission, Washington, D.C. (1975).
10. U.S. Nuclear Regulatory Commission, "Severe Accident Risks: An Assessment for Five U.S. Nuclear Power Plants," NUREG-1150, U.S. Nuclear Regulatory Commission, Washington, D.C. (1990).
11. Marseguerra, M., E. Zio, J. Devooght, and P.E. Labeau, "A Concept Paper on Dynamic Reliability via Monte Carlo Simulation," *Mathematics and Computers in Simulation*, **Volume 47**, pages 371-382 (1998).
12. Marseguerra, M., E. Zio, "Monte Carlo Approach to PSA for Dynamic Process Systems," *Reliability Engineering and System Safety*, **Volume 52**, pages 227-241 (1996).
13. Devooght J., C. Smidts, "Probabilistic Dynamics as a Tool for Dynamic PSA," *Reliability Engineering and System Safety*, **Volume 52**, pages 185-196 (1996).
14. Hofer E., M. Kloos, B. Krzykacs-Hausmann, J. Peschke, and M. Woltereck, "An Approximate Epistemic Uncertainty Analysis Approach in the Presence of Epistemic and Aleatory Uncertainties," *Reliability Engineering & System Safety*, **Volume 77**, pages 229-238 (2002).

15. Zhu, D., Y.H. Chang, and A. Mosleh, "The Use of Distributed Computing for Dynamic PRA: The ADS Approach," University of Maryland, College Park, MD (2008).
16. Nejad, H.S., A. Mosleh, "SimPRA: A Simulation-Based Probabilistic Risk Assessment Framework for Dynamic Systems," University of Maryland, College Park, MD (2007).
17. U.S. Nuclear Regulatory Commission, "Issues and recommendations for Advancement of PRA Technology in Risk-Informed Decision Making," NUREG/CR-6813, U.S. Nuclear Regulatory Commission, Washington D.C. (2003).
18. U.S. Nuclear Regulatory Commission, "Evaluation of Severe Accident Risks: Methodology for the Containment, Source Term, Consequence, and Risk Integration Analyses," NUREG/CR-4551, U.S. Nuclear Regulatory Commission, Washington D.C. (1993).
19. U.S. Nuclear Regulatory Commission, "MELCOR Computer Code Manuals," NUREG/CR-6119, Vol.2, Rev. 3 (SAND2005-5713), U.S. Nuclear Regulatory Commission, Washington, D.C. (2005).
20. U.S. Nuclear Regulatory Commission, "Code Manual for MACCS2, User's Guide," NUREG/CR-6613, U.S. Nuclear Regulatory Commission, Washington, D.C. (1998).
21. U.S. Nuclear Regulatory Commission, "Reevaluation of Station Blackout Risk at Nuclear Power Plants," NUREG/CR-6890, U.S. Nuclear Regulatory Commission, Washington D.C. (2005).
22. Kumar, R.K., G.W. Koroll, M. Heitsh, E. Studer, "Carbon Monoxide – Hydrogen Combustion Characteristics in Severe Accident Containment Conditions," NEA/CSNI/R(2000)10, Nuclear Energy Agency, France (2000).
23. Kim, J.Y., C.H. Chung, "Analysis of the Molten Core-Concrete Interactions under Severe Accidents with MELCOR Calculations," *Proceedings of the 7th International Conference on Nuclear Engineering*, Tokyo, Japan, April 19-23, paper ICONE-7816 (1999).
24. LeChateller, H., O. Boudouard, "On the Flammable Limits of Gas Mixtures," Bull Soc Chim (1898).
25. Coward, H.F., G.W. Jones, "Limits of Flammability of Gases and Vapors," Bulletin 503, Bureau of Mines, Washington D.C. (1952).
26. Bradfute, J.O., M.P. Paulsen, "Hydrogen Flammability Model Based on Present Data," Proceedings of the Workshop on the Impact of Hydrogen on Water Reactor Safety, Volume III, Albuquerque, NM (1981).
27. Sherman, M.P., M. Berman, R.F. Beyer, "Experimental Investigation of Pressure and Blockage Effects on Combustion Limits in H_2-Air-Steam Mixtures," SAND91-0252, Sandia National Laboratories, Albuquerque, NM (1993).
28. Rice, J.A., "*Mathematical Statistics and Data Analysis*," Third Edition, Brooks/Cole Cengage Learning, Belmont, CA (2007).
29. Sandia National Laboratories, NUREG/CR-7110 Volume 1, "State-of-the-Art Reactor Consequence Analyses Project Volume 1: Peach Bottom Integrated Analysis," U.S. Nuclear Regulatory Commission, Washington D.C. (2012).

30. Sandia National Laboratories, NUREG/CR-7110 Volume 2, "State-of-the-Art Reactor Consequence Analyses Project Volume 2: Surry Integrated Analysis," U.S. Nuclear Regulatory Commission, Washington D.C. (2012).
31. U.S. Nuclear Regulatory Commission, "Containment Integrity Research at Sandia National Laboratories," NUREG/CR-6906, U.S. Nuclear Regulatory Commission, Washington D.C. (2006).
32. U.S. Nuclear Regulatory Commission, "Pretest Prediction Analysis and Posttest Correlation of Sizewell-B 1:10 Scale Pre-stressed Concrete Containment Model Test, NUREG/CR-5671," U.S. Nuclear Regulatory Commission, Washington D.C. (1998).
33. Dameron, R.A., Y.R. Rashid, H.T. Tang, "Leak area and leakage rate prediction for probabilistic risk assessment of concrete containments under severe core conditions," *Nuclear Engineering and Design*, **Volume 156**, pages 173-179 (1995).